

LETTER TO THE EDITOR

Massive open star clusters using the VVV survey

III. A young massive cluster at the far edge of the Galactic bar[★]

S. Ramírez Alegría^{1,2}, J. Borissova^{1,2}, A.N. Chené³, E. O’Leary³, P. Amigo^{1,2}, D. Minniti^{2,4}, R. K. Saito⁵, D. Geisler⁶, R. Kurtev^{1,2}, M. Hempel^{2,4}, M. Gromadzki¹, J. R. A. Clarke¹, I. Negueruela⁷, A. Marco⁷, C. Fierro^{1,8}, C. Bonatto⁹, and M. Catelan^{2,4}

¹ Instituto de Física y Astronomía, Universidad de Valparaíso, Av. Gran Bretaña 1111, Playa Ancha, Casilla 5030, Valparaíso, Chile
e-mail: sebastian.ramirez@uv.cl

² The Millennium Institute of Astrophysics (MAS), Santiago, Chile

³ Gemini North Observatory, USA

⁴ Pontificia Universidad Católica de Chile, Instituto de Astrofísica, Av. Vicuña Mackenna 4860, 782-0436 Macul, Santiago, Chile

⁵ Universidade Federal de Sergipe, Departamento de Física, Av. Marechal Rondon s/n, 49100-000, São Cristóvão, SE, Brazil

⁶ Departamento de Astronomía, Casilla 160-C, Universidad de Concepción, Chile

⁷ Departamento de Física, Ingeniería de Sistemas y Teoría de la Señal, Universidad de Alicante, Spain

⁸ Escuela Superior de Física y Matemáticas del Instituto Politécnico Nacional, Unidad Profesional Adolfo López Mateos, México

⁹ Universidade Federal do Rio Grande do Sul, Departamento de Astronomia, CP 15051, RS, 91501-970 Porto Alegre, Brazil

Preprint online version: February 28, 2022

ABSTRACT

Context. Young massive clusters are key to map the Milky Way’s structure, and near-IR large area sky surveys have contributed strongly to the discovery of new obscured massive stellar clusters.

Aims. We present the third article in a series of papers focused on young and massive clusters discovered in the VVV survey. This article is dedicated to the physical characterization of VVV CL086, using part of its OB-stellar population.

Methods. We physically characterized the cluster using JHK_s near-infrared photometry from ESO public survey VVV images, using the VVV-SkZ pipeline, and near-infrared K -band spectroscopy, following the methodology presented in the first article of the series.

Results. Individual distances for two observed stars indicate that the cluster is located at the far edge of the Galactic bar. These stars, which are probable cluster members from the statistically field-star decontaminated CMD, have spectral types between O9 and B0 V. According to our analysis, this young cluster ($1.0 \text{ Myr} < \text{age} < 5.0 \text{ Myr}$) is located at a distance of 11_{-6}^{+5} kpc, and we estimate a lower limit for the cluster total mass of $(2.8_{-1.4}^{+1.6}) \cdot 10^3 M_{\odot}$. It is likely that the cluster contains even earlier and more massive stars.

Key words. Stars: early-types, massive - Techniques: photometric, spectroscopic - Galaxy: Disk, open clusters and associations: individual VVV CL086.

1. Introduction

Young massive clusters (cluster mass $M > 10^3 M_{\odot}$, ?) are fundamental pieces for the study of Galactic structure. Because of their youth, they give information related to the recent Galactic massive stellar formation history. They are also excellent tracers of star formation regions.

In the Milky Way, we find regions with intense stellar formation activity in the Galactic centre, where the Arches (Nagata et al. 1993; Figer et al. 2002), Center (Krabbe et al. 1995; Paumard et al. 2006; Figer 2008), and the Quintuplet (Glass et al. 1990; Okuda et al. 1990; Nagata et al. 1990; Figer et al. 1999) clusters are located; in the Carina-Sagittarius arm, which hosts Westerlund 2 (Westerlund 1961; Rauw et al. 2007; Ascenso et al. 2007a), Trumpler 14 (Ascenso et al. 2007b; Sanchawala et al. 2007; Sana et al. 2010), and NGC 3603 (Goss & Radhakrishnan 1969; Harayama et al. 2008);

and the close edge of the Galactic bar. In the last region, several clusters with a massive population of red supergiant (RSG) stars are found: RSGC1 (Figer et al. 2006; Davies et al. 2008), RSGC2 (Davies et al. 2007), RSGC3 (Alexander et al. 2009; Clark et al. 2009), Alicante 7 (Negueruela et al. 2010), Alicante 8 (Negueruela et al. 2011), and Alicante 10 (González-Fernández & Negueruela 2012), but also younger clusters with a mixed population of OB-type and RSG stars (Masgomas-1, Ramírez Alegría et al. 2012). By symmetry, we expect massive star clusters at the far edge of the Galactic bar. Until now, only one massive cluster is known in this region: Mercer 81 (Davies et al. 2012).

Owing to the distance and extinction expected for stars located at the far edge of the bar, clusters in that region must be observed with near-infrared filters, which are less affected by interstellar extinction, and with a high spatial resolution, to be able to resolve the distant cluster population. One of the most recent near-IR surveys, the ESO public survey VISTA Variables in the Vía Láctea (VVV, Minniti et al. 2010; Saito et al. 2010, 2012), is a perfect tool for this exploration, covering the Galactic bulge

[★] Based on observations taken within the ESO VISTA Public Survey VVV (programme ID 179.B-2002), and with ISAAC, VLT, ESO (programme 087.D-0341A).

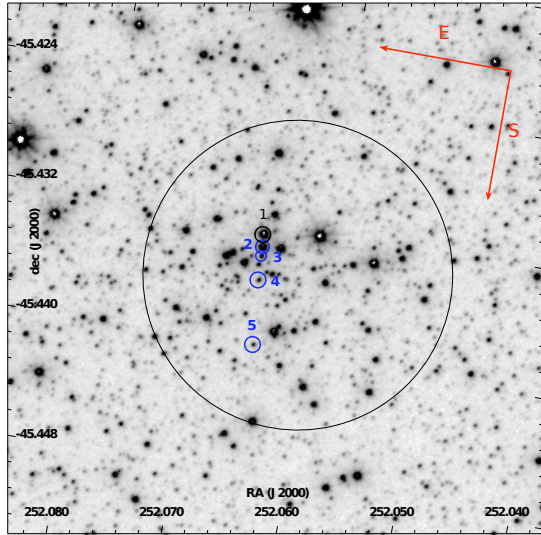


Fig. 1. VVV K_S image for VVV CL086. The image is 2×2 arcmin² size and the cluster radius of $35''$ (Borissova et al. 2011) is shown with a black circle. Small blue (OB-type stars) and black circles mark the position of the spectroscopically observed stars.

and the adjacent disk region, including the far edge of the bar with a spatial resolution of 0.34 arcsec pix^{-1} in $ZYJHK_S$ filters.

We present infrared spectrophotometric observations for VVV CL086 (Borissova et al. 2011), a massive cluster found in the direction of the Perseus arm ($l = 340^\circ 001$, $b = -0^\circ 293$), similar to that of Mercer 81 ($l = 338^\circ 400$, $b = +0^\circ 100$). Data observation and reduction are described in Section 2, near-IR photometry (CMD) and spectroscopy (spectral classification) are presented in Section 3. Cluster physical characterization is the topic of Section 4, and the general conclusions are given in the final Section 5.

2. Observations

The photometric data used in this work are part of the ESO Public Survey VVV, which observes with the VIRCAM at the VISTA telescope. VIRCAM has a 16-detector array (each detector with a 2048×2048 pixel size), and a pixel scale of 0.34 arcsec pix^{-1} . The gaps between the detectors are covered with a series of vertical and horizontal shifts, described in detail by Saito et al. (2012), but basically, six pawprints with a sky coverage of 0.59 square degrees, are combined into a single tile with a 1.64 square degrees field of view.

We obtained the photometry for our analysis using the VVV-SkZ pipeline (Mauro et al. 2013), an automated software based on ALLFRAME (Stetson 1994), and optimized for VISTA PSF photometry. We measured the J and H photometry over the stacked images, observed on 27 March, 2010, each with an exposure time of 40 seconds and downloaded from the VISTA Science Archive (VSA) website. The K_S photometry was calculated directly from the stacked images, observed between 6 June, 2010 and 1 July, 2013 (36 images). Photometric errors are lower than 0.2 mag for $K_S < 18$ mag, and for saturated bright stars ($K_S < 9.5$ mag) we used 2MASS photometry.

We also spectroscopically observed five stars that are marked with circles in Figure 1 with a single slit in the spectral range $2.03 - 2.34 \mu\text{m}$ with a resolution of $R \sim 3000$, using ISAAC at the Very Large Telescope at ESO Paranal Observatory, Chile (on 5

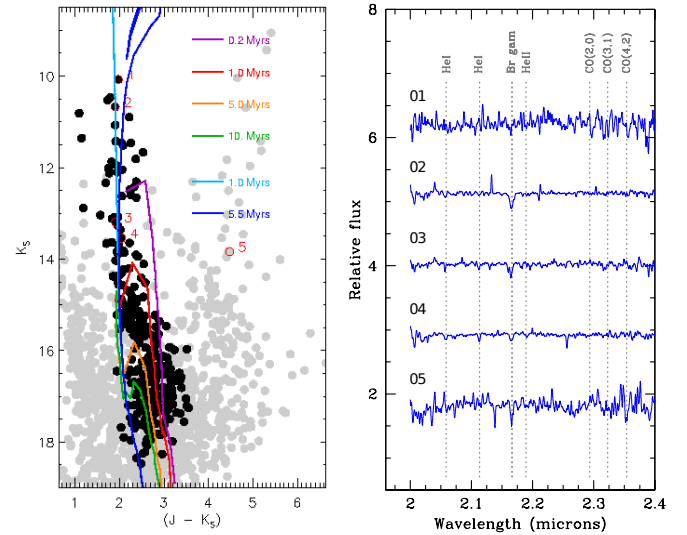


Fig. 2. *Left:* VVV CL086 field-star decontaminated CMD. The most probable cluster members and field stars are shown with black and grey symbols. Numbers indicate the position of the spectroscopically observed stars. Main (1.0 and 5.5 Myr, Lejeune & Schaerer 2001) and pre-main sequence (0.2, 1.0, 5.0, and 10 Myr, Siess et al. 2000) isochrones are also shown in the diagram. *Right:* individual spectra in K band for VVV CL086. We label the spectral lines used for the spectral classification.

May, 2011). The stars were observed using an ABBA observing mode to later subtract the atmospheric OH emission lines. For telluric standards we observed bright A0 V stars with similar airmass as the cluster stars.

For spectroscopic data reduction (flat-fielding, sky subtraction, spectra extraction, and wavelength calibration) we used the Interactive Data Language (IDL) and IRAF¹ scripts, following a similar procedure to that described by Chené et al. (2012). For the wavelength calibration we used the OH line, because of sudden shifts along the spectral dispersion direction during the observing night.

3. Results

In Figure 2 we present the $(J - K_S)$ vs. K_S colour-magnitude diagram. The diagram is statistically field-star decontaminated for a circle of radius 0.75 arcmin, centered around $\alpha_{2000} = 252^\circ 0651$, $\delta_{2000} = -45^\circ 4346$. The decontamination was performed as described by Borissova et al. (2011), using the algorithm of Bonatto & Bica (2010). The algorithm divides the K_S , $(H - K_S)$ and $(J - K_S)$ ranges into a grid of cells with sizes $\Delta K_S = 1.0$ mag, and $\Delta(J - K_S) = \Delta(H - K_S) = 0.2$ mag. In each cell, it estimates the expected number density of cluster stars by subtracting the respective field-star number density and, summing over all cells, it obtains a total number of member stars, N_{mem} . Grid shifts of $\pm 1/3$ the cell size are applied in each axes, producing 729 independent setups and N_{mem} . The average of these 729 N_{mem} (or $\langle N_{mem} \rangle$) is the limit for considering a star as a possible cluster member. Only the $\langle N_{mem} \rangle$ with highest survival frequency after all tests were finally considered as cluster members. To ensure photometric quality, the algorithm rejects

¹ IRAF is distributed by the National Optical Astronomy Observatories, which are operated by the Association of Universities for Research in Astronomy, Inc., under cooperative agreement with the National Science Foundation.

Table 1. Individual extinction and distance estimates for stars with spectral classification. Equatorial coordinates, near-infrared magnitudes (J , H , and K_S), and spectral classifications are given for all stars (except star #01, see Section 3). All reported errors are at the $1\text{-}\sigma$ level.

ID	RA (J2000) [deg]	dec (J2000) [deg]	J [mag]	H [mag]	K_S [mag]	ST	A_K [mag]	Distance [kpc]
01	252.06556	-45.43283	12.05±0.01	10.68±0.01	10.08±0.00(3)
02	252.06546	-45.43363	12.58±0.01	11.28±0.02	10.67±0.00(3)	B2–3 V	1.33±0.03	1.7 $^{+1.7}_{-0.4}$
03	252.06539	-45.43422	15.10±0.02	13.78±0.02	13.19±0.00(3)	O9–B0 V	1.38 $^{+0.02}_{-0.04}$	10.4 $^{+3.2}_{-5.0}$
04	252.06527	-45.43570	15.59±0.02	14.22±0.01	13.54±0.00(3)	O9 V	1.48 $^{+0.01}_{-0.10}$	11.7 $^{+3.4}_{-3.3}$
05	252.06481	-45.43973	18.31±0.03	15.15±0.01	13.83±0.00(3)	B0 V	3.06±0.03	6.2 $^{+1.1}_{-2.9}$

stars with uncertainties in K_S and colours larger than 0.2 mag. For comparison fields we used two concentric rings, centred on VVV CL086, with inner radius of 0.8' and 2.5', and outer radius of 1.2' and 5.0', and two circles with radius 1.4': one centred on $\alpha_{2000} = 252^{\circ}024$, $\delta_{2000} = -45^{\circ}48$ and the second centred on $\alpha_{2000} = 252^{\circ}110$, $\delta_{2000} = -45^{\circ}37$. The stellar densities were corrected for the area difference. The shape and size of the control field were chosen based on the distribution of stars and extinction clouds on the image.

In the field-decontaminated diagram we see that stars #01, #02, #03 and #04 are probably cluster members. Stars #03 and #04 are located in the cluster main sequence, but would not be the most massive stars in VVV CL086. Observed magnitudes and colours for the cluster stellar population appear to be affected by differential extinction, a characteristic commonly found in young massive clusters. From its location star #05, excluded as possible cluster member, is expected to be a foreground and very young star, reddened by its surrounding natal gas.

Spectral classification is based on the detection of absorption or emission lines (Bry, He I at 2.06, 2.11 μm , and He II at 2.19 μm) and the comparison of their shape and depth with similar-resolution spectral catalogues: Hanson et al. (1996) (K band) and Hanson et al. (1998) (H band) for OB-type stars. We assumed an error of ± 2 subtypes for the assigned spectral type, similar to Hanson et al. (2010) and Negueruela et al. (2010). The observed spectra and the lines used for the spectral classification are shown in Figure 2.

For spectrum #01 we do not detect any clear spectral feature. The spectrum is very noisy and probably presents faint ^{12}CO (2,0) bands at 2.29 μm . Even if the position of this star in the CMD is consistent with cluster membership, the faint CO band head indicates that star #01 is a very late type object.

Star #02 presents a clear Bry line in absorption and He I at 2.06 μm . Its Bry fits the B2 V HD19734 and B3 V HD201254 Bry lines. We adopted spectral type B2–3V for this star. Spectra #03 and #04 both show weak Bry and clear He I absorption line at 2.11 μm . For star #03, the lines fit the O9 V HD193322 and B0.5 V HD36960 spectra. For star #04 we also detected the He I line at 2.06 μm , and He II line at 2.19 μm , indicating that this star is of earlier type than star #03. Spectrum #04 fits O8.5 V HD73882, and O9 V HD193322 lines. For star #03 we adopted a spectral type between O9 and B0 V and for star #04, spectral type O9 V. Finally the spectrum of star #05 presents an absorption Bry line that fits a B0 V spectrum.

4. Discussion

4.1. Extinction, distance, and radial velocity

For individual distance estimates we compared the apparent magnitude with the intrinsic magnitude corresponding to each individual spectral type. We adopted the Rieke et al. (1989) extinction law, with $R = 3.09$ (Rieke & Lebofsky 1985), and intrinsic magnitudes and colours from Martins et al. (2005). For stars later than O9.5 V, we used the intrinsic magnitudes and colours from Cox (2000). Distance errors are dominated by the spectral type uncertainty, and we estimated it by deriving the individual distance for the same star assuming ± 2 spectral subtypes.

In Table 1 we present the individual extinction and distance determinations for the spectroscopically observed stars. Although the position of star #02 in the CMD associates it with the cluster population, its individual distance estimate indicates that it is a foreground star. Using the average of individual distances for stars #03 and #04 and the error propagation method described by Barlow (2004), we obtain a cluster distance of 11^{+5}_{-6} kpc. This would locate the cluster in the same region as Mercer 81, a massive cluster found at 11 ± 2 kpc (Davies et al. 2012). The mean extinction value for VVV CL086, $A_K = 1.5^{+0.0(3)}_{-0.1}$ is lower than the extinction value of $A_{2.22} = 2.5 \pm 0.5$ reported for Mercer 81 and indicates the possible presence of an extinction window in that galactic direction.

We measured the radial velocities with the IRAF tasks FXCOR and RVIDLINES for all the stars with spectral type determination. We used the He I at 2.076 and 2.11 μm and the Bry lines for the estimates. In all cases we measured negative RV, which is expected for the cluster direction, but the dispersion due to the number of used spectral lines and the signal-to-noise ratio from our spectra does not allow us to obtain a reliable estimate for stellar radial velocities.

4.2. Mass and age estimates

To estimate the total cluster mass, we first constructed the cluster present-day mass function using the CMD and then integrated the Kroupa (Kroupa 2001) initial mass function (IMF) fitted to the cluster IMF. Because we did not detect evolved stars, we assumed that the present-day and initial mass functions are equivalent.

We obtained the cluster present-day mass function by projecting all CMD stars, following the reddening vector, to the main sequence located at 11 kpc. The main sequence is defined by the colours and magnitudes given by Cox (2000). After deriving the cluster present-day luminosity function, using 1 K_S -mag bins, we converted the K_S magnitudes to solar masses using values from Martins et al. (2005) for O-type stars and from Cox (2000) for stars later than O9.5 V.

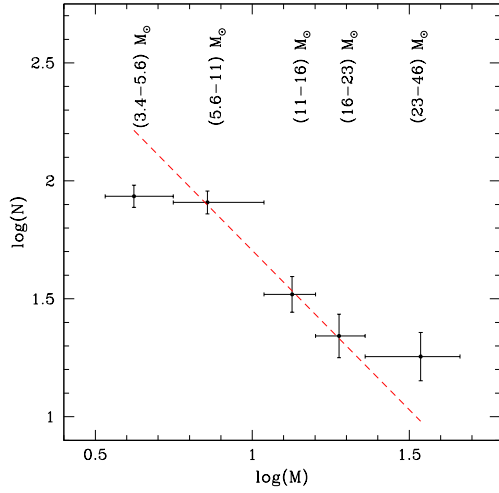


Fig. 3. VVV CL086 present-day mass function. The points show the central position in the mass ranges indicated above them, and the segmented red line corresponds to the Kroupa IMF fitted to the data. Bar sizes indicate the mass bin equivalent to each magnitude bin (from the luminosity function) of 1 mag in K_S .

The present-day mass function, shown in Figure 3, is fitted by a Kroupa (Kroupa 2001) IMF and integrated between 0.10 ($\log(M) = -1.00$ dex) and $35 M_{\odot}$ ($\log(M) = 1.54$ dex). For the cluster VVV CL086 we obtain a total mass of $(2.8^{+1.6}_{-1.4}) \cdot 10^3 M_{\odot}$. In our analysis we only included errors associated to the fitting of the Kroupa IMF to the data. In the cluster mass function we can see that the cluster could contain a more massive population than that spectroscopically detected by us (i.e. stars earlier than O9-B0 V), but the errors are large and dominated by small number statistics. Future spectroscopic observations will help to characterize this population and improve the mass estimate.

We tried to determine the cluster age by fitting main sequence (Lejeune & Schaerer 2001) and pre-main sequence (Siess et al. 2000) isochrones. However, young (i.e. younger than 10 Myr) cluster main sequences in the infrared are basically vertical lines, which prevented us from deriving a precise age for VVV CL086. Nonetheless, we observe the pre-main sequence turn-on point in the CMD. Pre-main sequence isochrones fitting indicates that the cluster age is > 1.0 and < 5.0 Myr.

5. Conclusions

We presented the physical characterization of VVV CL086, a new massive cluster discovered using data from the VVV survey, found at the far edge of the Milky Way bar at a distance of 11^{+5}_{-6} kpc. This cluster is the second one found in that region of the Galaxy (the first is Mercer 81), a region highly reddened by gas and dust, which presents a relatively low mean reddening of $A_K = 1.5^{+0.0(3)}_{-0.1}$ mag, however.

Our spectroscopic follow-up aimed at the brightest stars in the cluster area revealed that two objects are part of the disk population (two early-B dwarfs), and two stars form part of the cluster main-sequence population. From their spectral classification and the cluster CMD we were able to deduce that earlier stars than these two observed OB-stars are probably be present in VVV CL086. One star from our spectroscopic follow-up was not classified.

The mass estimate was derived by integrating the Kroupa IMF fitted to our data and gives a lower limit for the cluster total mass of $(2.8^{+1.6}_{-1.4}) \cdot 10^3 M_{\odot}$. We also estimated the cluster age by

fitting isochrones to the pre-main sequence turn-on point. We estimated a cluster age > 1.0 and < 5.0 Myr. The upper age limit agrees with the earliest main sequence star found in the cluster (i.e. O9 V star #04). Future spectroscopic observations are planned to confirm this and to investigate the cluster massive population in more detail.

Acknowledgements. We thank to the anonymous referee for the useful comments and suggestions, which helped us to improve this Letter. S.R.A. and A.N.C. were supported by the GEMINI-CONICYT project number 32110005. S.R.A. was also supported by the FONDECYT project No. 3140605. The VVV Survey is supported by ESO, by BASAL Center for Astrophysics and Associated Technologies PFB-06, by FONDAP Center for Astrophysics 15010003, and by the Ministry for the Economy, Development, and Tourism's Programa Inicativa Científica Milenio through grant IC 12009, awarded to The Millennium Institute of Astrophysics (MAS). Support for J.B. is provided by FONDECYT Regular No.1120601, P.A. acknowledges the support by ALMA-CONICYT project number 31110002 and D.M., from FONDECYT No. 1130196. M.G. is financed by the GEMINI-CONICYT Fund, allocated to Project 32110014. D.G. gratefully acknowledges support from the Chilean BASAL Centro de Excelencia en Astrofísica y Tecnologías Afines (CATA) grant PFB-06/2007. R.K.S. acknowledges partial support from FONDECYT through grant 1130140, and CNPq/Brazil through projects 310636/2013-2 and 481468/2013-7. M.C. acknowledges additional support from FONDECYT through grants #1110326 and 1141141. The work of I.N. and A.M. is partially supported by the Spanish Ministerio de Economía y Competitividad (Mineco) under grant AYA2012-39364-C02-02.

This publication makes use of data products from the Two Micron All Sky Survey, which is a joint project of the University of Massachusetts and the Infrared Processing and Analysis Center/California Institute of Technology, funded by the National Aeronautics and Space Administration and the National Science Foundation.

References

- Alexander, M. J., Kobulnicky, H. A., Clemens, D. P., et al. 2009, *AJ*, 137, 4824
 Ascenso, J., Alves, J., Beletsky, Y., & Lago, M. T. V. T. 2007a, *A&A*, 466, 137
 Ascenso, J., Alves, J., Vicente, S., & Lago, M. T. V. T. 2007b, *A&A*, 476, 199
 Barlow, R. 2004, [arXiv:physics/0406120]
 Bonatto, C. & Bica, E. 2010, *A&A*, 516, A81
 Borissova, J., Bonatto, C., Kurtev, R., et al. 2011, *A&A*, 532, A131
 Chené, A.-N., Borissova, J., Clarke, J. R. A., et al. 2012, *A&A*, 545, A54
 Clark, J. S., Negueruela, I., Davies, B., et al. 2009, *A&A*, 498, 109
 Cox, A. N. 2000, *Allen's Astrophysical Quantities*, 4th edition (Springer, New York)
 Davies, B., de La Fuente, D., Najarro, F., et al. 2012, *MNRAS*, 419, 1860
 Davies, B., Figer, D. F., Kudritzki, R.-P., et al. 2007, *ApJ*, 671, 781
 Davies, B., Figer, D. F., Law, C. J., et al. 2008, *ApJ*, 676, 1016
 Figer, D. F. 2008, in *IAU Symposium*, Vol. 250, *IAU Symposium*, ed. F. Bresolin, P. A. Crowther, & J. Puls, 247–256
 Figer, D. F., Kim, S. S., Morris, M., et al. 1999, *ApJ*, 525, 750
 Figer, D. F., MacKenty, J. W., Robberto, M., et al. 2006, *ApJ*, 643, 1166
 Figer, D. F., Najarro, F., Gilmore, D., et al. 2002, *ApJ*, 581, 258
 Glass, I. S., Moneti, A., & Moorwood, A. F. M. 1990, *MNRAS*, 242, 55P
 González-Fernández, C. & Negueruela, I. 2012, *A&A*, 539, A100
 Goss, W. M. & Radhakrishnan, V. 1969, *Astrophys. Lett.*, 4, 199
 Hanson, M. M., Conti, P. S., & Rieke, M. J. 1996, *ApJS*, 107, 281
 Hanson, M. M., Kurtev, R., Borissova, J., et al. 2010, *A&A*, 516, A35
 Hanson, M. M. & Popescu, B. 2008, in *IAU Symposium*, Vol. 250, *IAU Symposium*, ed. F. Bresolin, P. A. Crowther, & J. Puls, 307–312
 Hanson, M. M., Rieke, G. H., & Luhman, K. L. 1998, *AJ*, 116, 1915
 Harayama, Y., Eisenhauer, F., & Martins, F. 2008, *ApJ*, 675, 1319
 Krabbe, A., Genzel, R., Eckart, A., et al. 1995, *ApJ*, 447, L95
 Kroupa, P. 2001, *MNRAS*, 322, 231
 Lejeune, T. & Schaerer, D. 2001, *A&A*, 366, 538
 Martins, F., Schaerer, D., & Hillier, D. J. 2005, *A&A*, 436, 1049
 Mauro, F., Moni Bidin, C., Chené, A.-N., et al. 2013, *Rev. Mexicana Astron. Astrofis.*, 49, 189
 Minniti, D., Lucas, P. W., Emerson, J. P., et al. 2010, *New Astronomy*, 15, 433
 Nagata, T., Hyland, A. R., Straw, S. M., Sato, S., & Kawara, K. 1993, *ApJ*, 406, 501
 Nagata, T., Woodward, C. E., Shure, M., Pipher, J. L., & Okuda, H. 1990, *ApJ*, 351, 83
 Negueruela, I., González-Fernández, C., Marco, A., & Clark, J. S. 2011, *A&A*, 528, A59

- Negueruela, I., González-Fernández, C., Marco, A., Clark, J. S., & Martínez-Núñez, S. 2010, *A&A*, 513, 74
- Okuda, H., Shibai, H., Nakagawa, T., et al. 1990, *ApJ*, 351, 89
- Paumard, T., Genzel, R., Martins, F., et al. 2006, *ApJ*, 643, 1011
- Ramírez Alegría, S., Marín-Franch, A., & Herrero, A. 2012, *A&A*, 541, A75
- Rauw, G., Manfroid, J., Gosset, E., et al. 2007, *A&A*, 463, 981
- Rieke, G. H. & Lebofsky, M. J. 1985, *ApJ*, 288, 618
- Rieke, G. H., Rieke, M. J., & Paul, A. E. 1989, *ApJ*, 336, 752
- Saito, R., Hempel, M., Alonso-García, J., et al. 2010, *The Messenger*, 141, 24
- Saito, R. K., Hempel, M., Minniti, D., et al. 2012, *A&A*, 537, A107
- Sana, H., Momany, Y., Gieles, M., et al. 2010, *A&A*, 515, A26
- Sanchawala, K., Chen, W.-P., Ojha, D., et al. 2007, *ApJ*, 667, 963
- Siess, L., Dufour, E., & Forestini, M. 2000, *A&A*, 358, 593
- Stetson, P. B. 1994, *PASP*, 106, 250
- Westerlund, B. 1961, *AJ*, 66, 57